Fibroblast growth factor receptor-1 phosphorylation requirement for cardiomyocyte differentiation in murine embryonic stem cells

Roberto Ronca [a, #], Laura Gualandi [a, #], Elisabetta Crescini [a], Stefano Calza [b], Marco Presta [a], Patrizia Dell'Era [a, *]

[a] Unit of General Pathology and Immunology, Department of Biomedical Sciences and Biotechnology, University of Brescia, Brescia, Italy
[b] Unit of Medical Statistics, Department of Biomedical Sciences and Biotechnology, University of Brescia, Brescia, Italy

Received: February 23, 2009; Accepted: June 1, 2009

Abstract

Fibroblast growth factor receptor-1 (*Fgfr1*) gene knockout impairs cardiac and haematopoietic development in murine embryonic stem cells (mESC). In FGFR1, tyrosine residues Y653 and Y654 are responsible for its tyrosine kinase (TK) activity whereas phosphorylated Y463 and Y766 represent docking sites for intracellular substrates. Aim of this study was the characterization of FGFR1 signalling requirements necessary for cardiomyocyte differentiation in mESC. To this purpose, *fgfr1*$^{-/-}$ mESC were infected with lentiviral vectors harbouring human wild-type hFGFR1 or the Y653/654F, Y463F and Y766F hFGFR1 mutants. The resulting embryonic stem (ES) cell lines were differentiated as embryoid bodies (EBs) and beating foci formation was evaluated. In order to appraise the presence of cells belonging to cardiovascular and haematopoietic lineages, specific markers were analysed by quantitative PCR, whole mount *in situ* hybridization and immunofluorescence. Transduction with TK^{+} hFGFR1 or the TK^{+} Y766F-hFGFR1 mutant rescued cardiomyocyte beating foci formation in *fgfr1*$^{-/-}$ EBs whereas the TK^{-} Y653/654F-hFGFR1 mutant and the TK^{+} Y463F-hFGFR1 mutant were both ineffective. Analysis of the expression of early and late cardiac markers in differentiating EBs confirmed these observations. At variance with cardiomyocyte differentiation, all the transduced TK^{+} FGFR1 forms were able to rescue haematopoietic differentiation in EBs originated by infected *fgfr1*$^{-/-}$ mESC, only the TK^{-} Y653/654F-hFGFR1 mutant being ineffective. In keeping with these observations, treatment with different signalling pathway inhibitors indicates that protein kinase C and ERK activation are essential for cardiomyocyte but not for haematopoietic differentiation in EBs generated by *fgfr1*$^{+/-}$ mESC. In conclusion, our results suggest that, although FGFR1 kinase activity is necessary for both cardiac and haematopoietic lineage maturation in mESC, phosphorylation of Y463 in the intracellular domain of the receptor is a specific requirement for cardiomyocyte differentiation.

Keywords: FGFR • embryonic stem cells • cardiomyocyte

Introduction

Heart is the first organ to be formed in vertebrate embryo development. Precardiac mesoderm cells become allocated at or shortly after gastrulation, leading to the formation of a single beating linear heart tube that undergoes right-ward looping followed by segmentation and growth of cardiac chambers [1]. Cardiac development involves several stages: early mesodermal differentiation, generation of cardiovascular common progenitors that can differentiate in cardiomyocytes, smooth muscle cells and endothelial cells [2–4], cardiac lineage commitment of cardiac progenitor (CP) cells and maturation of functional cardiomyocytes [5]. The classical view of cardiogenesis has been recently modified by the demonstration that two distinct mesodermal heart fields with a common origin contribute to heart development in a temporally and spatially specific manner [6]. The expression of *tbx5*, a T-box transcription factor that is initially expressed throughout the cardiac crescent, appears lately to be restricted to derivatives of the first/primary heart field (FHF) [6–8], whereas the progenitors of the secondary heart field (SHF) are characterized by the expression of *fgf10* and of the LIM domain homeobox gene *isl1* [9, 10]. Both FHF and SHF progenitors express instead the homeodomain transcription factor *nkx2.5* [6, 11].

[#] The first two authors contributed equally to this work.
*Correspondence to: Patrizia DELL'ERA,
Unit of General Pathology and Immunology,
Department of Biomedical Sciences and Biotechnology,
University of Brescia,
Viale Europa, 11, 25123 Brescia, Italy.
Tel.: +39-0303717539
Fax: +39-0303701157
E-mail: dellera@med.unibs.it; patrizia.dellera@gmail.com

doi: 10.1111/j.1582-4934.2009.00805.x

Most of these recent developmental findings involved the use of animal models paralleled by *in vitro* differentiation studies on murine embryonic stem cells (mESC). mESC originate from the inner cell mass of the blastocyst and are capable of cell renewal and differentiation after *in vitro* aggregation into three-dimensional structures termed embryoid bodies (EBs) [12, 13]. Cardiac development in mESC differentiation cultures is well established and is easily detected by the appearance of areas of contracting cells that display characteristics of mature cardiomyocytes [14]. All of the cardiac cell types have been generated from differentiating EBs, and gene expression analyses suggest that their development in culture recapitulates cardiogenesis in the early embryo [15, 16]. Indeed, CP cells originated from both FHF and SHF, characterized by the common expression of *nkx2.5* and by the selective expression of *tbx5* and *fgf10*/*isl1*, have been isolated from differentiating ESC populations [2, 3].

Fibroblast growth factor receptors (FGFRs) belong the subclass IV of membrane-spanning tyrosine kinase (TK) receptors [17]. Four *fgfr* genes have been identified: FGFR1–4 proteins share common structural features and interact with the members of the FGF family comprising of at least 23 polypeptides [18]. The FGF/FGFR system has been implicated in a variety of physiological and pathological conditions, including embryonic development, tissue growth and remodelling, inflammation, tumour growth and vascularization [19, 20]. Following ligand binding and receptor dimerization, a number of tyrosine autophosphorylation sites have been identified in human FGFR1 (hFGFR1): Y653/654 are critical for TK activity [21], Y463 is involved in endothelial cell proliferation by binding to Src homology (SH)2/SH3 domain-containing adaptor protein Crk [22] and phosphorylated Y766 has been shown to bind phospholipase C-γ (PLC-γ) in L6 myoblasts, Shb in endothelial cells and Grb14 in MDA-MB-231 human breast cancer cells [23–25]. Also, FGFR1 activation leads to FRS2 phosphorylation [26] followed by Grb2 and Shp2 interactions [27]. FRS2, Crk and Shb binding to FGFR1 affect the classical Ras/Raf-1/MEK/ERK/Jun proliferation pathway activated by TK receptors, while PLCγ1 activates protein kinase C (PKC) [28], whose role in cardiomyocyte differentiation has been demonstrated [29]. FGF/FGFR signalling plays important functions in mesoderm formation and development [30]. Accordingly, *fgfr1*$^{-/-}$ mice die during gastrulation, displaying defective mesoderm patterning with reduction in the amount of paraxial mesoderm and lack of somite formation [31, 32]. Studies on chimeric embryos using FGFR1-deficient mESC revealed an early defect in the mesodermal and endodermal cell movement through the primitive streak, followed by deficiencies in contributing to anterior mesoderm, including heart tissue [33, 34]. The pivotal contribution of FGF signalling in heart formation has been demonstrated in different animal models: in *C. intestinalis*, FGF signalling delineates the cardiac progenitor field [35]; in *Drosophila,* mesoderm spreading depends upon the expression of *heartless,* homologous to vertebrate *fgfr1,* and the *heartless* mutant is characterized by the absence of the heart [36, 37]; in chicken, FGF signalling activated by FGF8 contributes to the heart-inducing properties of the endoderm [38]; in zebrafish, induction and differentiation of the heart requires FGF8 [39]; in mice, *Fgf8*$^{neo/-}$ mutants show complex cardiac defects [40].

FGFR1 has been implicated in cardiac development also during murine EB differentiation. Indeed, analysis of the *in vitro* differentiation process of *fgfr1*$^{-/-}$ mESC following EB formation led us to determine a non-redundant role for FGFR1 in cardiomyocyte development [41]. Moreover, the FGFR1 TK inhibitor SU 5402 [42], the MEK1/2 inhibitor U0126 [43] and the classical/novel PKC inhibitor GF109203X [44] were all able to hamper beating foci formation in EBs originated by *fgfr1*$^{+/-}$ mESC, further implicating the FGFR1 TK activity, ERK and PKC in cardiomyocyte differentiation.

Here, in order to further define the requirements for FGFR1 signalling in cardiomyogenesis, *fgfr1*$^{-/-}$ mESC were transduced *via* a lentiviral vector system with hFGFR1 or with hFGFR1 forms mutated in different tyrosine autophosphorylation sites. Analysis of the differentiative capacity of EBs originated by the different mESC populations demonstrates the non-redundant role for the tyrosine autophosphorylation site Y463 in cardiomyocyte development. Y463 phosphorylation appears instead to be dispensable for haematopoietic differentiation, thus indicating that distinct FGFR1-dependent signalling pathways are required for cardiomyocyte and haematopoietic differentiation in mESC.

Materials and methods

ES cell culture

Murine ESC [32, 41] were adapted to grow without feeder cells and maintained in Dulbecco's Modified Eagle's Medium supplemented with 20% foetal bovine serum (Hyclone, South Logan, UT, USA), 0.1 mmol/l non-essential amino acids, 1 mmol/l sodium pyruvate, 0.1 mmol/l β-mercaptoethanol, 2 mmol/l L-glutamine and 1000 U/ml LIF (ESGRO, Millipore, Milan, Italy). At T_0 of differentiation, exponentially growing mESC were resuspended in LIF-deprived EB medium and cultured in 30 μl hanging drops (400 cells) for 2 days to allow cell aggregation. Then, aggregates were transferred onto 0.5% agarose-coated dishes and grown for 5 days in LIF-deprived EB medium. At day 7, EBs were transferred into 24-well tissue culture plates and allowed to adhere. Aggregates were monitored for the appearance of spontaneously contracting foci during the following days.

RNA extraction, semi-quantitative and quantitative RT-PCR analysis

Total RNA was extracted from mESC as described [45]. Contaminating DNA was digested using DNAse, following indications reported in RNeasy® Micro Handbook (Qiagen, Milan, Italy). Two μg of total RNA were retrotranscribed with MMLV reverse transcriptase (InVitrogen, Milan, Italy) using random hexaprimers in a final 20 μl volume. For semi-quantitative PCR, 2 μl of the retrotranscribed RNA were subjected to polymerase chain reaction (PCR) using REDTaq® ReadyMix™ PCR Reaction Mix (Sigma, Milan, Italy). Oligonucleotide primers and PCR conditions were described previously [41]. The data were confirmed by analysing RNA extracted from two or more independent differentiation experiments. Quantitative PCR was performed with a Biorad iCycler iQ™ Real-Time PCR Detection System

using a iQ™ SYBR Green Supermix (Biorad, Milan, Italy) according to manufacturer's instructions. The qPCR-specific primers (final concentration 400 nM) were as follows: *nkx2.5* forward (for) primer: 5′- CCAAGTGCTCTCCTGCTTTC; reverse (rev) primer: 5′- GTCCAGCTCCACTGCCTTCT; *myl2* for: 5′-AAAGAGGCTCCAGGTCCAAT; rev: 5′-CTGGTCGATCTCCTCTTTGG; *tubulin* for: 5′-CCGGACAGTGTGGCAACCAGATCGG; rev: 5′-TGGCCAAAAGGACCTGAGCGAACGG; *itga2b* for: 5′-TTCTTGGGTCCTAGTGCTGTT; rev: 5′- CGCTTCCATGTTTGTCCTTATGA; *fgf10* for: 5′-AAGGCTGTTCTCCTTCACCA; rev: 5′- CCCCTTCTTGTTCATGGCTA; *vcam1* for: 5′-GAACTGATTATCCAAGTCTCTCCA; rev: 5′- CCATGTCTCCTGTCTTTGCTT; *ptprc* for: 5′- CAATGGAGTGTACGAGGGAGA; rev: 5′-CATCCATCAGCTGCTTTTCA; *hbb-bh1* for: 5′-ACTCTGGGAAGGCTCCTGAT; rev: 5′-CCCAAGGATGTCAGCACTTT. Gene expression levels were evaluated by comparing differentiated cells to the relative undifferentiated state. Data were analysed using REST [46]; statistical significance was evaluated by means of linear mixed models.

Vector production and transduction

Human FGFR1, Y653/654F-hFGFR1, Y463F-hFGFR1 and Y766F-hFGFR1 cDNAs [47] were independently cloned in the transfer vector pRRL-SIN-PPT-hPGK-GFP-WPRE by replacing green fluorescent protein (GFP) gene [48]. Viral particles were produced, purified by ultracentrifugation and used to infect murine *fgfr1*$^{-/-}$ mESC, following a standard protocol [48, 49]. As a control experiment, *fgfr1*$^{+/-}$ and *fgfr1*$^{-/-}$ mESC were infected with lentiviruses harbouring GFP under the ubiquitous phosphoglycerate kinase promoter [48]. In both cell types, GFP expression was observed in more than 90% of the undifferentiated cells and was maintained throughout the whole experimental differentiation protocol (data not shown). Moreover, GFP transduction did not affect beating foci formation in *fgfr1*$^{+/-}$ EBs (data not shown).

Binding assay and immunoblot analysis

^{125}I-FGF2 binding assay was described previously [45]. Briefly, human recombinant FGF2 was labelled with ^{125}I (37 GBq/ml; GE Healthcare Life Science, Milan, Italy) using Iodogen (Pierce, Rockford, IL, USA) at a specific radioactivity equal to 1800 cpm/fmol. mESC were seeded in 24-well dishes at the density of 250,000 per cm^2 in complete medium. After 24 hrs, a standard binding assay was performed using 3 ng/ml ^{125}I-FGF2 in the absence or in the presence of an excess of unlabelled FGF2. At the end of the incubation, cells were washed with 2 M NaCl, 20 mM Hepes, pH 7.2. Then, radioactivity bound to high-affinity sites was stripped with 20 mM sodium acetate, pH 4, and measured in a gamma-counter (Wallac, Waltham, MA, USA).

For immunoblot analysis mESC were seeded at 200,000 cells/cm^2 and starved in 1% FCS overnight. Then, cells were stimulated with FGF2 (100 ng/ml) for 15 min. and directly lysed in reducing sample buffer. Samples were run on 10% SDS-PAGE and transferred to Immobilon-P (Millipore, Milan, Italy). $ERK_{1/2}$ phosphorylation was evaluated by membrane incubation with anti-phospho-$ERK_{1/2}$ antibody (sc-7383, Santa Cruz Biotechnology Inc.), while uniform loading was judged by incubation of the same membrane with anti-ERK_2 antibody (sc-1647, Santa Cruz Biotechnology Inc., Santa Cruz, CA, USA).

Whole mount *in situ* hybridization (WISH)

Total RNA from *fgfr1*$^{+/-}$ EBs at day 10 of differentiation was reverse transcribed to cDNA and used as template for PCR reactions using the following oligonucleotide primers: *myl2* for: 5′-GCCAAGAAGCGGATAGAAGG; rev: 5′-CTGTGGTTCAGGGCTCAGTC; *cdh5* for: 5′-TTTGGAATCAAATGCACATCGA; rev: 5′-TGCTGTACTTGGTCATCCGGTT. Fragments were subcloned into pCR®II-TOPO® vector (InVitrogen). The plasmids were linearized and used as template for RNA synthesis with T7 or SP6 polymerase for antisense and sense control probes in the presence of digoxigenin-11-UTP by using DIG RNA labelling kit (Roche Diagnostics, Milan, Italy).

At day 10 of differentiation, EBs were fixed overnight in 4% paraformaldehyde (PFA) in phosphate-buffered saline (PBS), dehydrated with methanol 100% and stored at –20°C until hybridization. Fixed EBs were rehydrated and rinsed twice in PBS, 0.1% Tween® 20 (PBT), then digested with proteinase K (10 μg/ml in PBT) for 15 min. at room temperature, followed by incubation in 4% PFA in PBS for 20 min. EBs were subsequently rinsed twice in PBT for 5 min. and pre-hybridized at 65°C in hybridization mix (HM: 50% formamide, 5× SSC, 10 mM citric acid pH 6, 0.1% Tween® 20, 50 μg/ml heparin, 50 μg/ml tRNA) for 2 hrs. EBs were then incubated overnight at 65°C in HM containing 1 μg/ml of denatured riboprobe. On the second day, EBs were sequentially washed in 2× SSC containing 75%, 50%, 25% and 0% of hybrizidation wash (50% formamide, 5× SSC, 10 mM citric acid pH 6, 0.1% Tween® 20) at 65°C for 15 min. each, followed by three washes with 0.2× SSC at 65°C for 30 min. EBs were then rinsed at room temperature with increasing concentrations of PBT (25%, 50% and 75%, respectively, 10 min. each) in 0.2× SSC, incubated for 3 hrs in blocking buffer (BB: 2% sheep serum, 2 mg/ml BSA in PBT), and immunodecorated overnight at 4°C in BB containing 1:10,000 alkaline phosphatase-coupled anti-digoxigenin antibody (Roche Diagnostics). On the following day, EBs were extensively washed with PBT and the reaction was developed in staining solution [100 mM Tris HCl pH 9.5, 50 mM $MgCl_2$, 100 mM NaCl, 0.1% Tween® 20, 500 μM Tetramisole, NBT and BCIP (Roche Diagnostics)] following manufacturer's instruction. Hybridized EBs were post-fixed for 20 min. in 4% PFA in PBS and subsequently dehydrated and included in paraffin. Seven μM sections were cut, mounted with DPX (Fluka, Milan, Italy), observed and photographed under a Zeiss Axiophot2 stereomicroscope.

Immunostaining

EBs were grown from day 7 of differentiation in LabTek™ Chamber Slide™ System (Nunc, Rochester, NY, USA). At day 10 of differentiation, they were fixed overnight at 4°C in zinc fix (0.1 M Tris HCl, pH 7.5, 3 mM calcium acetate, 23 mM zinc acetate and 37 mM zinc chloride). After blocking unspecific binding in 3% BSA for 1 hr at room temperature, EBs were incubated overnight at 4°C with primary mouse anti-troponin T monoclonal antibody (Abcam, Cambridge, UK). The following day, EBs were washed for 30 min. with 10 mM Tris HCL, pH mM NaCl (TBS) and incubated for 1 hr at room temperature with secondary FITC-conjugated anti-mouse IgG (Fab specific) (Sigma Aldrich). EBs were washed in DAPI-containing TBS and then photographed with a Zeiss Axiovert 200M microscope.

Results and discussion

Transduction of hFGFR1 in murine *fgfr1*$^{-/-}$ mESC

Analysis of the *in vitro* differentiation process of *fgfr1*$^{+/-}$ and *fgfr1*$^{-/-}$ mESC following EBs formation had shown that FGFR1 is

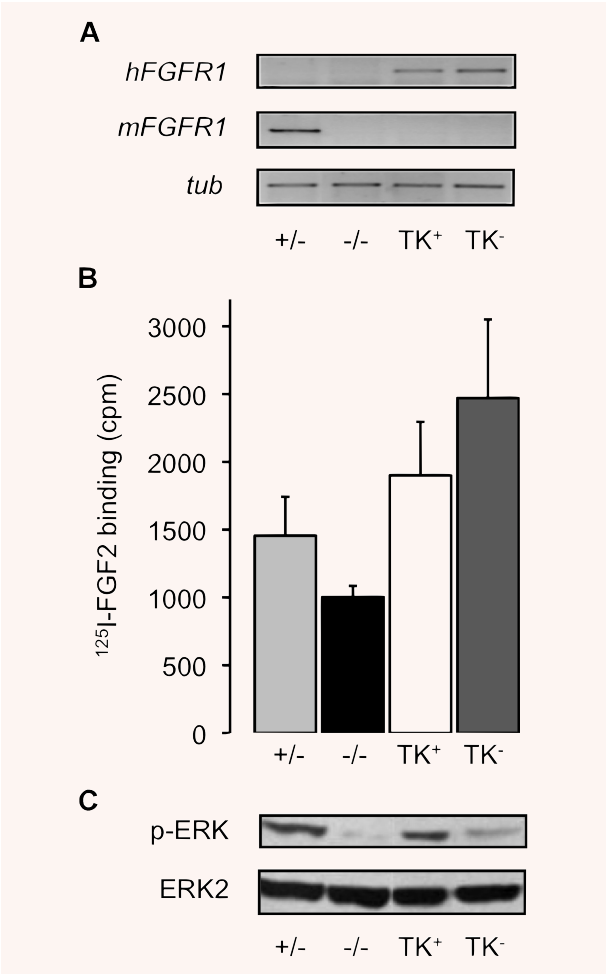

Fig. 1 Characterization of *fgfr1*$^{-/-}$ mESC transduced with TK^{+} or TK^{-} hFGFR1. *Fgfr1*$^{-/-}$ mESC were infected with a lentiviral vector carrying either TK^{+} (wt) or TK^{-} Y653/654F-hFGFR1 cDNAs. (**A**) Total RNA was extracted from *fgfr1*$^{+/-}$ (+/–), *fgfr1*$^{-/-}$ (–/–), and the infected mESC populations v-wt-hFGFR1 (TK^{+}), and v-Y653/654F-hFGFR1 (TK^{-}). Equivalent amounts of cDNA were amplified by PCR using the indicated primers. The *tubulin* gene was used for normalization. (**B**) *fgfr1*$^{+/-}$ (+/–), *fgfr1*$^{-/-}$ (–/–), v-wt-hFGFR1 (TK^{+}) and v-Y653/654F-hFGFR1 (TK^{-}) mESC were seeded at 250,000 cells/cm^2 and incubated for 2 hr at 4°C with ^{125}I-FGF2. At the end of the incubation, cells were washed and radioactivity bound to high-affinity sites was evaluated . Data represent the mean of at least four independent experiments ± S.D. (**C**) *fgfr1*$^{+/-}$ (+/–), *fgfr1*$^{-/-}$ (–/–), v-wt-hFGFR1 (TK^{+}) and v-Y653/654F-hFGFR1 (TK^{-}) mESC were seeded at 200,000 cells/cm^2 and starved in 1% FCS overnight. Then, cells were stimulated with FGF2 (100 ng/ml) for 15 min. and directly lysed in reducing sample buffer. Samples were loaded on 10% SDS-PAGE and processed for Western blot analysis. ERK$_{1/2}$ phosphorylation was evaluated by incubation with anti-phospho-ERK$_{1/2}$ antibody (sc-7383, Santa Cruz Biotechnology Inc.), while uniform loading was judged by incubation of the same membrane with anti-ERK$_2$ antibody (sc-1647, Santa Cruz Biotechnology Inc.).

essential for cardiomyocyte differentiation [41]. The human FGFR1 gene product shares 98% amino acid sequence identity with the murine counterpart. Most of the differences between the two molecules are located in the first Ig-like loop of the extracellular domain, a region dispensable for the specificity of FGFs-FGFR1 interaction [50, 51]. The aminoacidic identity of murine and human FGFR1 raises to 100% in the intracellular domain that comprises all the tyrosine autophosphorylation sites [21, 51]. On this basis, to get further insights about the role of FGFR1 signalling in cardiomyocyte differentiation, we cloned wild-type TK^{+} [49] and the mutant TK^{-} Y653/654F [21] hFGFR1 cDNAs into pRRL.sin.PPT.hPGK.GFPpre vector [48] by replacing the GFP gene. The high-titre vesicular stomatitis virus-pseudotyped lentiviral particles carrying hFGFR1 cDNAs were collected from supernatant of 293T-transfected cells and used to infect *fgfr1*$^{-/-}$ mESC, thus generating v-wt-hFGFR1 and v-Y653/654F-hFGFR1 mESC populations. Because of the high transfection efficiency ($>$ 90%, data not shown), the entire infected populations were used for further characterization. hFGFR1 expression by infected cells was evaluated by semi-quantitative RT-PCR analysis and ^{125}I-FGF2 binding assay. As anticipated, infected *fgfr1*$^{-/-}$ mESC lines show amplified transcripts for hFGFR1 but lack the endogenous murine counterpart (Fig. 1A). Moreover, infected cells show an increase in high-affinity ^{125}I-FGF2 binding when compared with control cells (Fig. 1B), indicating that both TK^{+} and TK^{-}-transduced receptors are exposed on the cell surface. It must be pointed out that a certain amount of high-affinity ^{125}I-FGF2 binding was observed also in *fgfr1*$^{-/-}$ mESC, probably due to the ability of FGF2 to bind other FGFRs [52]. Finally, to assess the signalling capacity of the transduced receptors, undifferentiated ES cell populations were stimulated with exogenous recombinant FGF2 and ERK$_{1/2}$ phosphorylation was evaluated by Western blotting. As shown in Fig. 1C, significant levels of activated ERK$_{1/2}$ were observed in FGF2-stimulated *fgfr1*$^{+/-}$ mESC and in *fgfr1*$^{-/-}$ mESC transduced with the TK^{+} hFGFR1, but not in non-infected *fgfr1*$^{-/-}$ mESC and in *fgfr1*$^{-/-}$ mESC transduced with the TK^{-} Y653/654F-hFGFR1 mutant. On this basis, we assessed the capacity of TK^{+} hFGFR1 and TK^{-} Y653/654F-hFGFR1 to rescue cardiomyocyte differentiation in the mESC *fgfr1* knockout background.

Cardiomyocyte differentiation in TK^{+} and TK^{-} hFGFR1 transduced *fgfr1*$^{-/-}$ mESC

At day 7 of differentiation, EBs derived from the different mESC populations were allowed to adhere to the substratum and monitored during the following days for the appearance of spontaneously contracting foci (Fig. 2A). As anticipated, a high percentage of *fgfr1*$^{+/-}$ EBs generates pulsating cardiomyocytes 1 day after attachment whereas *fgfr1*$^{-/-}$ EBs show a dramatic decrease in this capacity. However, infection with TK^{+} hFGFR1 restores the capacity of *fgfr1*$^{-/-}$ EBs to originate beating cells, although the kinetics of their appearance showed a slight delay in respect to *fgfr1*$^{+/-}$ mESC. At variance, this capacity was completely hampered in TK^{-} Y653/654F-hFGFR1 EBs.

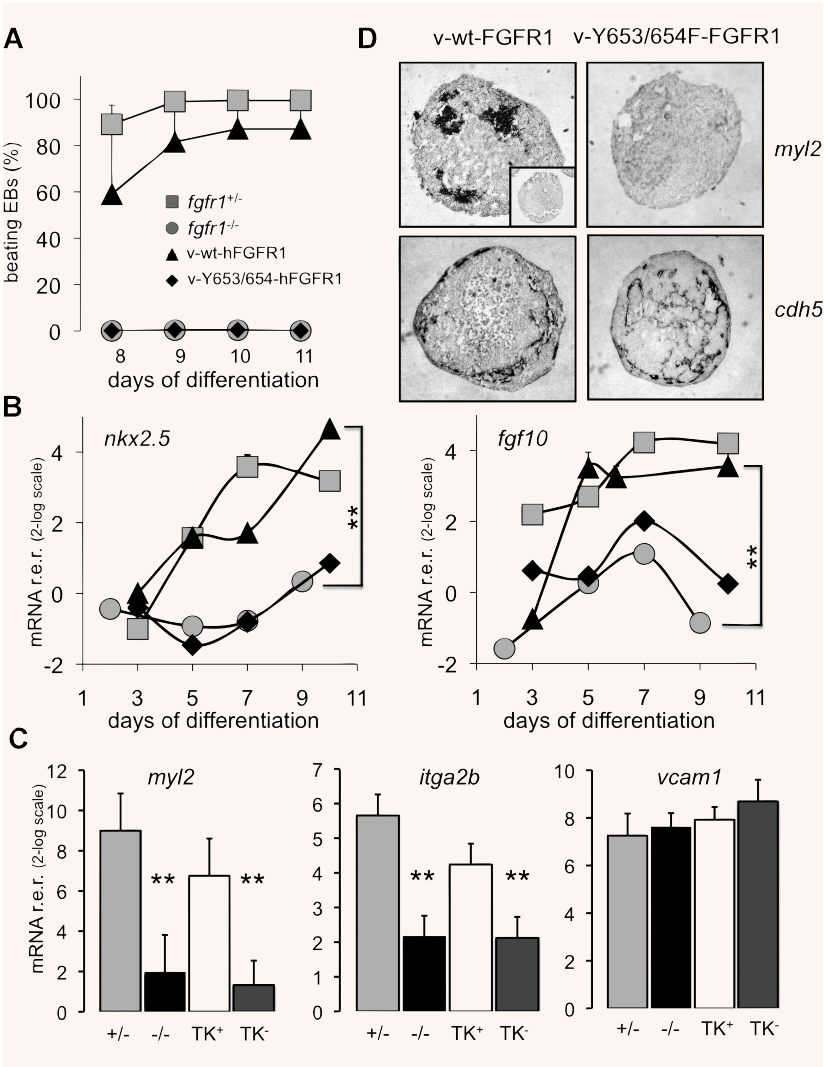

Fig. 2 Cardiomyocyte formation during differentiation of TK^+ and TK^- hFGFR1 mESC. (**A**) *Fgfr1*$^{+/-}$, *fgfr1*$^{-/-}$, and the infected v-wt-hFGFR1 and v-Y653/654F-hFGFR1 mESC were subjected to standard differentiation protocol and the percentage of EBs with spontaneously contracting foci were counted under an inverted microscope. Data represent the mean of at least four independent experiments. (**B**) *Fgfr1*$^{+/-}$ (grey squares), *fgfr1*$^{-/-}$ (grey circles), and the infected v-wt-hFGFR1 (black triangles) and v-Y653/654F-hFGFR1 mESC (black lozenges) were subjected to standard differentiation protocol. Then, total RNA was extracted, retrotranscribed and subjected to qPCR reaction using the indicated primers. Gene expression levels were quantified using REST [46] by comparing differentiated cells to the relative undifferentiated state. Data are expressed as relative expression ratio (r.e.r.) with error bars representing the mean ± S.E. **, $P < 0.005$. (**C**) Total RNA was extracted from *fgfr1*$^{+/-}$ (+/–), *fgfr1*$^{-/-}$ (–/–), v-wt-hFGFR1 (TK^+) and v-Y653/654F-hFGFR1 (TK^-) EBs at day 10 of differentiation. Equivalent amounts of cDNA were amplified by qPCR using the indicated primers. Gene expression levels were quantified using REST [46] by comparing differentiated cells to the relative undifferentiated state. Data are expressed r.e.r. with error bars representing the mean ± S.E. **, $P < 0.005$. (**D**) Whole mount *in situ* hybridization of v-wt-hFGFR1 and v-Y653/654F-hFGFR1 EBs at day 10 of differentiation using *myl2* and *cdh5* antisense probes as indicated. The insert in the top left panel shows hybridization of the same EBs with the control *myl2* sense probe. Data are representative of at least two independent experiments with an average number of 10 EBs for each hybridization.

Previous observations had shown that differentiating *fgfr1*$^{-/-}$ EBs do not express the transcription factor *nkx2.5*, a marker of cardiac progenitors of both FHF and SHF [5, 41]. On this basis, to assess the effect of transduced TK^+ hFGFR1 and TK^- Y653/654F-hFGFR1 on the block of cardiomyocyte differentiation in *fgfr1*$^{-/-}$ mESC, total RNA was extracted from differentiating EBs and analysed for the expression of *nkx2.5* and *fgf10* by quantitative PCR (qPCR), using the relative undifferentiated state as reference sample. As shown in Fig. 2B, *nkx2.5* is strongly up-regulated in *fgfr1*$^{+/-}$ EBs from day 3 of differentiation, whereas its expression remains at very low levels in *fgfr1*$^{-/-}$ EBs until day 9. Transduction of TK^+ hFGFR1 in *fgfr1*$^{-/-}$ EBs restores the up-regulation of *nkx2.5* expression to levels similar to those observed in *fgfr1*$^{+/-}$ EBs, while transduction of the TK^- hFGFR1 mutant is ineffective. Similar results were obtained for *fgf10* expression: again, a significant up-regulation of *fgf10* expression was observed in EBs generated by *fgfr1*$^{+/-}$ and v-wt-hFGFR1 mESC but not by v-Y653/654F-hFGFR1 mESC (Fig. 2B).

We had previously demonstrated that the expression of the cardiogenic mesodermal marker *mef2c* is not affected in differentiating *fgfr1* knockout mESC [41]. Since Mef2c cooperates with Nkx2.5 and other cardiac transcription factors in inducing downstream effectors [53], we hypothesized that FGFR1 may mediate cardiomyocyte differentiation by activating Nkx2.5 in $Mef2c^+$ cardiogenic mesodermal cells. The present data confirm the non-redundant role of FGFR1 in *nkx2.5* up-regulation and cardiomyocyte differentiation. However, in all our studies, the expression analysis of cardiac markers in differentiating mESC has been performed on the total RNA extracted from the whole EB. Considering that the expression of these markers is not always restricted to a single cell population, only the isolation of the different cardiomyocyte progenitor populations (reviewed in [5]) will allow the precise

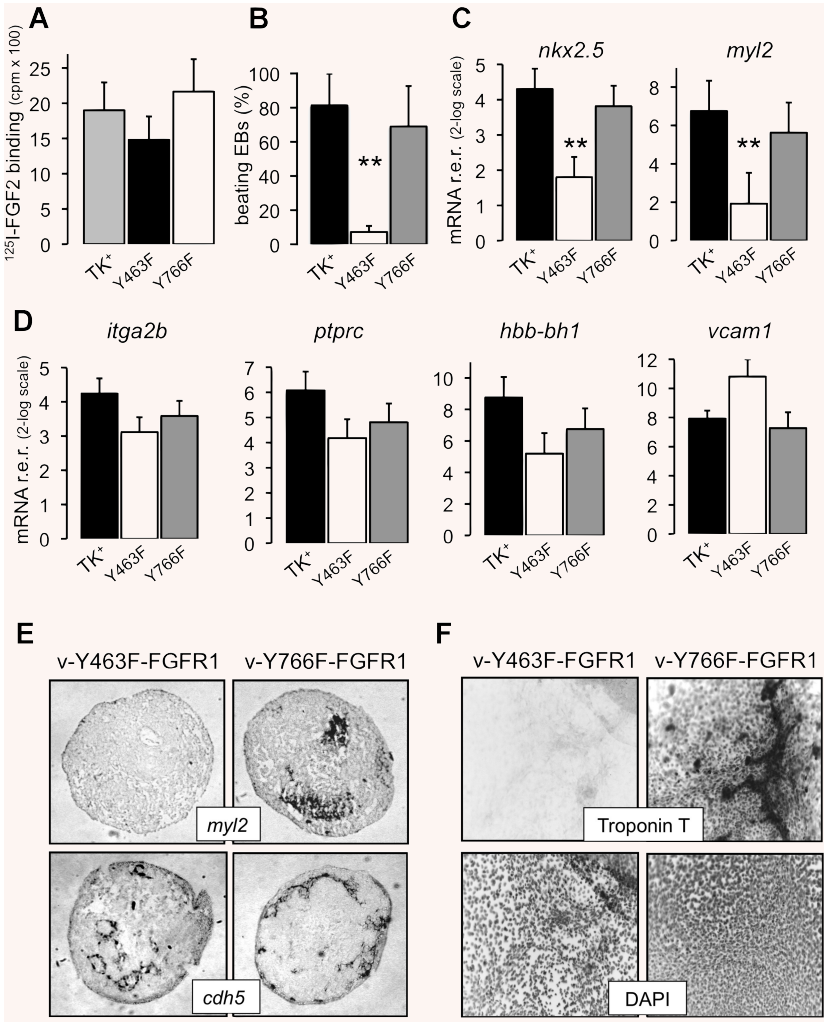

Fig. 3 Characterization of v-Y463F-hFGFR1 and v-Y766F-hFGFR1 mESC differentiation. (**A**) v-wt-hFGFR1 (TK$^+$), v-Y463F-hFGFR1 (Y463F) and v-Y766F-hFGFR1 (Y766F) mESC were seeded at 250,000 cells/cm^2 and incubated with ^{125}I-FGF2. Data represent the mean of at least four independent experiments. (**B**) v-wt-hFGFR1 (TK$^+$), v-Y463F-hFGFR1 (Y463F) and v-Y766F-hFGFR1 (Y766F) mESC were subjected to standard differentiation protocol and the percentage of EBs with spontaneously contracting foci were counted under an inverted microscope at day 10. Data represent the mean of at least four independent experiments. (**C, D**) Total RNA was extracted from v-wt-hFGFR1 (TK$^+$), v-Y463F-hFGFR1 (Y463F) and v-Y766F-hFGFR1 (Y766F) mESC populations at day 10 of differentiation. Equivalent amounts of cDNA were amplified by quantitative PCR using the indicated primers. Gene expression levels were quantified using REST [46] by comparing differentiated cells to the relative undifferentiated state. Data are expressed as r.e.r. with error bars representing the mean ± S.E. **, $P < 0.005$. (**E**) Whole mount *in situ* hybridization of v-Y463F-hFGFR1 and v-Y766F-hFGFR1 EBs at day 10 of differentiation. Data are representative of at least two independent experiments with an average number of 10 EBs for each hybridization. (**F**) Immunostaining of cardiac troponin T in v-Y463F-hFGFR1 and v-Y766F-hFGFR1 EBs at day 10 of differentiation. Nuclei were counterstained with DAPI. Magnification 200×.

identification of the step(s) in the cardiomyocyte differentiation pathway characterized by a non-redundant role for FGFR1. For instance, the FHF and SHF markers Tbx5 and Isl1, whose expression is not limited to heart tissue [54, 55], show similar up-regulation kinetics in *fgfr1*$^{+/-}$, *fgfr1*$^{-/-}$, and the infected v-wt-hFGFR1 and v-Y653/654F-hFGFR1 mESC populations (data not shown).

To further characterize differentiating transduced EBs, the expression of structural markers belonging to different lineages of mesodermal origin was evaluated by qPCR and whole mount *in situ* hybridization (WISH). FGFR1 is implicated in cardiac and haematopoietic development but is dispensable for endothelial cell differentiation in murine EBs [41, 49]. Accordingly, *fgfr1*$^{+/-}$ and TK$^+$ v-wt-hFGFR1 mESC, but not *fgfr1*$^{-/-}$ and TK$^-$ v-Y653/654F-hFGFR1 cells, express the cardiac ventricular myosin light chain (*myl2*) and the primitive haematopoietic marker CD41 (*itga2b*) at day 10 of differentiation (Fig. 2C and D). All the cell lines express instead the endothelial markers *vcam1* (Fig. 2C) and *vascular endothelial cadherin* (*cdh5*) (Fig. 2D) at similar levels.

Thus, viral transduction in a *fgfr1* null background of TK$^+$ hFGFR1, but not of the TK$^-$ Y653/654F hFGFR1 mutant, is sufficient to rescue the ability of mESC to undergo cardiomyocyte and haematopoietic differentiation.

Role of Y463 and Y766 FGFR1 residues in cardiomyocyte differentiation

Seven autophosphorylation sites have been identified in the cytoplasmic domain of hFGFR1 [21]. Among them, Y463 and Y766 represent docking sites for intracellular molecules. To assess the relative contribution of these residues in transducing signal(s) for cardiomyocyte development, we infected *fgfr1*$^{-/-}$ mESC with lentiviral particles harbouring the cDNA for the TK$^+$ hFGFR1 mutants Y463F or Y766F. Again, the efficient transduction of the receptor mutants was confirmed by RT-PCR (data not shown) and ^{125}I-FGF2 binding assay (Fig. 3A), whereas their TK$^+$ signalling

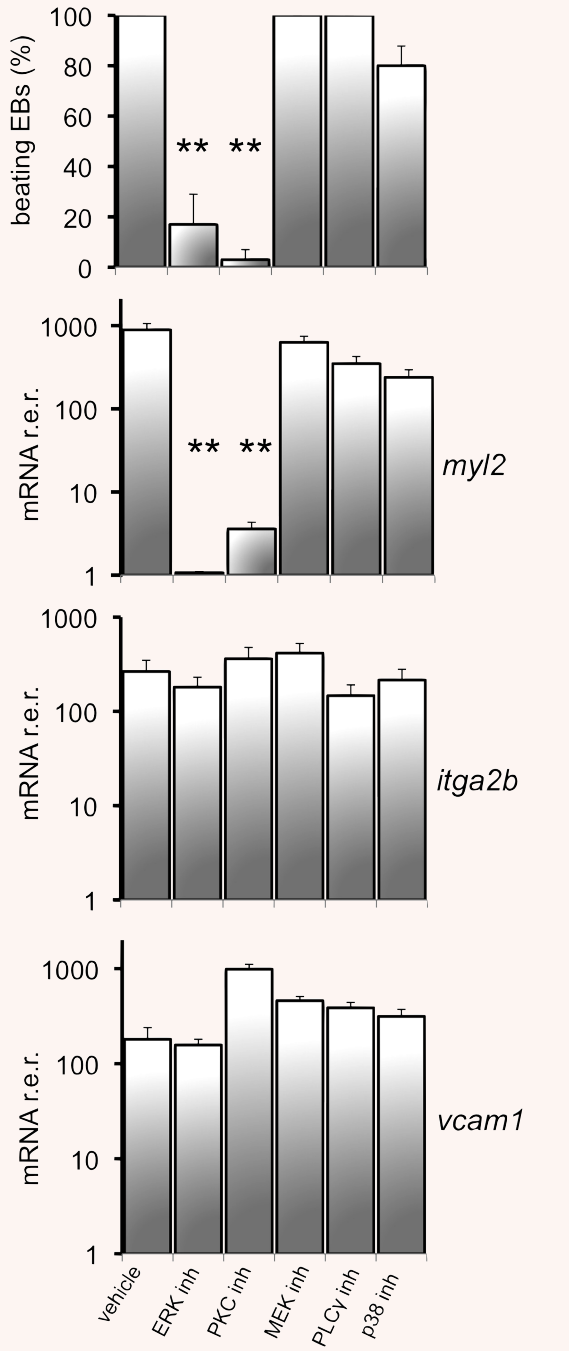

Fig. 4 Effect of signalling inhibitors on beating foci formation in *fgfr1*$^{+/-}$ EBs. *Fgfr1*$^{+/-}$ mESC were subjected to standard differentiation protocol. After LIF withdrawal, cells were incubated with vehicle (DMSO), 10 μM ERK inhibitor U0126, 2 μM PKC inhibitor GF109203X, 20 μM MEK inhibitor PD98059, 5 μM PLC-γ inhibitor U73122, or 3 μM p38 inhibitor SB203580. All the inhibitors were from Calbiochem (Merck, Darmstadt, Germany). Treatment was repeated on differentiation day 2. Beating foci formation was scored at day 10 and EBs were harvested for total RNA extraction. Equivalent amounts of cDNA were amplified by quantitative PCR using the indicated primers. Gene expression levels were quantified using REST [46] by comparing differentiated cells to the relative undifferentiated state. Data are expressed as r.e.r. with error bars representing the mean ± S.E. **, $P < 0.005$.

capacity was judged by FGF2-induced $ERK_{1/2}$ phosphorylation (data not shown). Next, v-Y463F-hFGFR1 and v-Y766F-hFGFR1 mESC underwent the standard differentiation protocol and the appearance of beating cardiomyocytes was monitored. At day 10 of differentiation, v-Y463F-hFGFR1 EBs showed a dramatic impairment in generating beating foci when compared to v-Y766F-hFGFR1 EBs whose ability was only marginally reduced in respect to v-wt-hFGFR1 EBs (Fig. 3B). In agreement with the microscopic observations, analysis of Y463F-hFGFR1 EBs showed a strong reduction of the cardiac gene transcripts *nkx2.5* and *myl2* (Fig. 3C and E) and of cardiac structural protein troponin T (Fig. 3F). As expected, no down-regulation was seen in the levels of expression of the endothelial markers *vcam1* and *cdh5* (Fig. 3D and E).

Because of the involvement of FGFR1 in ES haematopoietic development (see above), v-Y463F-hFGFR1 and v-Y766F-hFGFR1 EBs were also evaluated for the expression of haematopoietic markers (Fig. 3D). In contrast with what observed for cardiac markers, the transcript levels of the primitive integrin *itga2b*, of the pan tyrosine phosphatase CD45 (*ptprc*), and of the embryonic beta-like globin gene *hbb-bh1* were similar in v-Y463F-hFGFR1 and v-Y766F-hFGFR1 EBs and comparable to those detected in v-wt-hFGFR1 EBs. Thus, our data strongly suggest that Y463 residue in FGFR1 is specifically involved in cardiomyocyte differentiation of mESC. Moreover, this residue, together with residue Y766, is dispensable for FGFR1-mediated haematopoietic development.

We have previously observed that beating cardiomyocyte differentiation in *fgfr1*$^{+/-}$ EBs can be hampered by $ERK_{1/2}$ and PKC inhibitors [44]. To get further insights about the signalling cascade that leads to cardiomyocyte differentiation in mESC and to assess the possibility to dissociate cardiac and haematopoietic differentiation at pharmacological level, as suggested by distinct tyrosine autophosphorylation requirements in FGFR1, differentiating *fgfr1*$^{+/-}$ EBs were treated with different signalling inhibitors and assessed for the expression of lineage-specific markers (Fig. 4). In keeping with previous observations [41], beating foci formation and the expression of the structural cardiac marker *myl2* were strongly reduced by 10 μM $ERK_{1/2}$ inhibitor U0126 [43] or by 2 μM PKC inhibitor GF109203X [44], whereas the expression of the haematopoietic marker *itga2b* and of the endothelial marker *vcam1* were not affected. Moreover, MEK inhibitor PD98059 [56], PLC-γ inhibitor U73122 [57], or p38 inhibitor SB203580 [58], when used at the recommended concentrations of 20 μM [59], 5 μM [60] and 3 μM [61], respectively, did not affect any of the differentiation processes investigated (Fig. 4). No inhibition in beating foci formation was obtained also when the same inhibitors were added at higher non-toxic concentrations, like 50 μM for

PD98059 and 20 μM for both U73122 and SB 203580 (data not shown). Thus, the data confirm the role of $ERK_{1/2}$ and PKC signalling in cardiomyocyte formation and indicate that different signalling requirements are involved in FGFR1-dependent haematopoietic differentiation.

Phosphorylation of Y463 in FGFR1 leads to the Crk-mediated activation of the Ras/Raf-1/MEK/ERK/Jun pathway in endothelial cells [22], whereas Y766 phosphorylation activates PLC-γ in myoblasts and triggers the hydrolysis of phosphatidylinositols that, in turn, stimulate PKC [62]. The ability of the Y766-hFGFR1 mutant to restore cardiomyocyte differentiation in transduced *fgfr1*$^{-/-}$ mESC and the lack of inhibitory effect of the PLC-γ inhibitor U73122 on the appearance of beating foci in *fgfr1*$^{+/-}$ EBs rule out a role for PLC-γ in the PKC-dependent pathway involved in cardiomyocyte formation [29]. On the other hand, the ability of the $ERK_{1/2}$ inhibitor U0126, but not of the MEK inhibitor PD98059, to hamper beating foci formation in *fgfr1*$^{+/-}$ EBs as well as in *fgfr1*$^{-/-}$ EBs treated with the PKC activator phorbol miristate acetate [41] suggests that $ERK_{1/2}$ activation required for cardiomyocyte differentiation is triggered by a PKC-dependent pathway rather than by the classical Ras/Raf-1/MEK pathway that FGFR1 dimerization activates in NIH3T3 fibroblasts [63]. Indeed, ERK2 can be activated by several PKC isoforms in Swiss 3T3 fibroblasts [29], including the novel PKC δ and ε isoforms involved in cardiomyocyte differentiation [64]. Clearly, the possibility exists that PKC and ERK pathways may play complementary roles at different times and/or in different cell types during EB differentiation.

At present, the signalling cascade triggered by the autophosphorylation of Y463 in FGFR1 and its cross-talk with PKC- and ERK-mediated signalling during cardiomyocyte differentiation of mESC remains to be elucidated. Indeed, Western blot analysis of total EB protein extract at day 9 of differentiation does not show any difference in CrkII and Shp2 phosphorylation levels among *fgfr1*$^{-/-}$, v-wt-hFGFR1, v-Y463F-hFGFR1 and v-Y653/654F-hFGFR1 EBs, thus indicating that the overall activation of these signalling molecules in differentiating EBs is not restricted to FGFR1 activity (data not shown). Also, FRS2 appears to be phosphorylated in both v-Y463F-hFGFR1 and v-wt-hFGFR1 EBs but not in TK^{-} v-Y653/654F-hFGFR1 and *fgfr1*$^{-/-}$ EBs, indicating that its activation depends on the TK activity of FGFR1 but not on Y463 phosphorylation (data not shown). Again, only the isolation of the different cardiomyocyte progenitor populations from these EBs will allow the identification of the FGFR1-dependent signalling pathway(s) involved in cardiomyocyte differentiation in mESC. Nevertheless, our data demonstrate for the first time a specific non-redundant role for residue Y463 of FGFR1 in cardiomyocyte differentiation.

Acknowledgements

We thank Michele De Palma and Luigi Naldini (San Raffaele Scientific Institute, Milan, Italy) for kind gift of the lentiviral expression system. This work was supported by Centro per lo Studio del Trattamento dello Scompenso Cardiaco (University of Brescia); Istituto Superiore di Sanità (Oncotechnological Program); Ministero dell'Istruzione, Università e Ricerca (Centro di Eccellenza per l'Innovazione Diagnostica e Terapeutica, Cofin projects); Associazione Italiana per la Ricerca sul Cancro; Fondazione Berlucchi; and NOBEL Project Cariplo to M.P.

References

1. **Mohun T, Sparrow D.** Early steps in vertebrate cardiogenesis. *Curr Opin Genet Dev.* 1997; 7: 628–33.
2. **Kattman SJ, Huber TL, Keller GM.** Multipotent flk-1+ cardiovascular progenitor cells give rise to the cardiomyocyte, endothelial, and vascular smooth muscle lineages. *Dev Cell.* 2006; 11: 723–32.
3. **Moretti A, Caron L, Nakano A, *et al.*** Multipotent embryonic isl1+ progenitor cells lead to cardiac, smooth muscle, and endothelial cell diversification. *Cell.* 2006; 127: 1151–65.
4. **Wu SM, Fujiwara Y, Cibulsky SM, *et al.*** Developmental origin of a bipotential myocardial and smooth muscle cell precursor in the mammalian heart. *Cell.* 2006; 127: 1137–50.
5. **Chen K, Wu L, Wang ZZ.** Extrinsic regulation of cardiomyocyte differentiation of embryonic stem cells. *J Cell Biochem.* 2008; 104: 119–28.
6. **Buckingham M, Meilhac S, Zaffran S.** Building the mammalian heart from two sources of myocardial cells. *Nat Rev Genet.* 2005; 6: 826–35.
7. **Bruneau BG, Nemer G, Schmitt JP, *et al.*** A murine model of Holt-Oram syndrome defines roles of the T-box transcription factor Tbx5 in cardiogenesis and disease. *Cell.* 2001; 106: 709–21.
8. **Zaffran S, Kelly RG, Meilhac SM, *et al.*** Right ventricular myocardium derives from the anterior heart field. *Circ Res.* 2004; 95: 261–8.
9. **Cai CL, Liang X, Shi Y, *et al.*** Isl1 identifies a cardiac progenitor population that proliferates prior to differentiation and contributes a majority of cells to the heart. *Dev Cell.* 2003; 5: 877–89.
10. **Kelly RG, Brown NA, Buckingham ME.** The arterial pole of the mouse heart forms from Fgf10-expressing cells in pharyngeal mesoderm. *Dev Cell.* 2001; 1: 435–40.
11. **Srivastava D.** Making or breaking the heart: from lineage determination to morphogenesis. *Cell.* 2006; 126: 1037–48.
12. **Nishikawa S, Jakt LM, Era T.** Embryonic stem-cell culture as a tool for developmental cell biology. *Nat Rev Mol Cell Biol.* 2007; 8: 502–7.
13. **Desbaillets I, Ziegler U, Groscurth P, *et al.*** Embryoid bodies: an *in vitro* model of mouse embryogenesis. *Exp Physiol.* 2000; 85: 645–51.
14. **Boheler KR, Czyz J, Tweedie D, *et al.*** Differentiation of pluripotent embryonic stem cells into cardiomyocytes. *Circ Res.* 2002; 91: 189–201.
15. **Maltsev VA, Rohwedel J, Hescheler J, *et al.*** Embryonic stem cells differentiate *in vitro* into cardiomyocytes representing sinusnodal, atrial and ventricular cell types. *Mech Dev.* 1993; 44: 41–50.
16. **Sachinidis A, Kolossov E, Fleischmann BK, *et al.*** Generation of cardiomyocytes

from embryonic stem cells experimental studies. *Herz.* 2002; 27: 589–97.
17. **Fantl WJ, Johnson DE, Williams LT.** Signalling by receptor tyrosine kinases. *Annu Rev Biochem.* 1993; 62: 453–81.
18. **Chen GJ, Forough R.** Fibroblast growth factors, fibroblast growth factor receptors, diseases, and drugs. *Recent Pat Cardiovasc Drug Discov.* 2006; 1: 211–24.
19. **Powers CJ, McLeskey SW, Wellstein A.** Fibroblast growth factors, their receptors and signaling. *Endocr Relat Cancer.* 2000; 7: 165–97.
20. **Presta M, Dell'Era P, Mitola S, *et al.*** Fibroblast growth factor/fibroblast growth factor receptor system in angiogenesis. *Cytokine Growth Factor Rev.* 2005; 16: 159–78.
21. **Mohammadi M, Dikic I, Sorokin A, *et al.*** Identification of six novel autophosphorylation sites on fibroblast growth factor receptor 1 and elucidation of their importance in receptor activation and signal transduction. *Mol Cell Biol.* 1996; 16: 977–89.
22. **Larsson H, Klint P, Landgren E, *et al.*** Fibroblast growth factor receptor-1-mediated endothelial cell proliferation is dependent on the Src homology (SH) 2/SH3 domain-containing adaptor protein Crk. *J Biol Chem.* 1999; 274: 25726–34.
23. **Mohammadi M, Honegger AM, Rotin D, *et al.*** A tyrosine-phosphorylated carboxy-terminal peptide of the fibroblast growth factor receptor (Flg) is a binding site for the SH2 domain of phospholipase C-gamma 1. *Mol Cell Biol.* 1991; 11: 5068–78.
24. **Cross MJ, Lu L, Magnusson P, *et al.*** The Shb adaptor protein binds to tyrosine 766 in the FGFR-1 and regulates the Ras/MEK/MAPK pathway *via* FRS2 phosphorylation in endothelial cells. *Mol Biol Cell.* 2002; 13: 2881–93.
25. **Cailliau K, Perdereau D, Lescuyer A, *et al.*** FGF receptor phosphotyrosine 766 is a target for Grb14 to inhibit MDA-MB-231 human breast cancer cell signaling. *Anticancer Res.* 2005; 25: 3877–82.
26. **Kouhara H, Hadari YR, Spivak-Kroizman T, *et al.*** A lipid-anchored Grb2-binding protein that links FGF-receptor activation to the Ras/MAPK signaling pathway. *Cell.* 1997; 89: 693–702.
27. **Hadari YR, Kouhara H, Lax I, *et al.*** Binding of Shp2 tyrosine phosphatase to FRS2 is essential for fibroblast growth factor-induced PC12 cell differentiation. *Mol Cell Biol.* 1998; 18: 3966–73.
28. **Hug H, Sarre TF.** Protein kinase C isoenzymes: divergence in signal transduction? *Biochem J.* 1993; 291: 329–43.
29. **Zhou X, Quann E, Gallicano GI.** Differentiation of nonbeating embryonic stem cells into beating cardiomyocytes is dependent on downregulation of PKC beta and zeta in concert with upregulation of PKC epsilon. *Dev Biol.* 2003; 255: 407–22.
30. **Xu X, Weinstein M, Li C, Deng C.** Fibroblast growth factor receptors (FGFRs) and their roles in limb development. *Cell Tissue Res.* 1999; 296: 33–43.
31. **Yamaguchi TP, Harpal K, Henkemeyer M, *et al.*** fgfr-1 is required for embryonic growth and mesodermal patterning during mouse gastrulation. *Genes Dev.* 1994; 8: 3032–44.
32. **Deng CX, Wynshaw-Boris A, Shen MM, *et al.*** Murine FGFR-1 is required for early postimplantation growth and axial organization. *Genes Dev.* 1994; 8: 3045–57.
33. **Ciruna BG, Schwartz L, Harpal K, *et al.*** Chimeric analysis of fibroblast growth factor receptor-1 (Fgfr1) function: a role for FGFR1 in morphogenetic movement through the primitive streak. *Development.* 1997; 124: 2829–41.
34. **Deng C, Bedford M, Li C, *et al.*** Fibroblast growth factor receptor-1 (FGFR-1) is essential for normal neural tube and limb development. *Dev Biol.* 1997; 185: 42–54.
35. **Davidson B.** Ciona intestinalis as a model for cardiac development. *Semin Cell Dev Biol.* 2007; 18: 16–26.
36. **Beiman M, Shilo BZ, Volk T.** Heartless, a *Drosophila* FGF receptor homolog, is essential for cell migration and establishment of several mesodermal lineages. *Genes Dev.* 1996; 10: 2993–3002.
37. **Frasch M.** Induction of visceral and cardiac mesoderm by ectodermal Dpp in the early *Drosophila* embryo. *Nature.* 1995; 374: 464–7.
38. **Alsan BH, Schultheiss TM.** Regulation of avian cardiogenesis by Fgf8 signaling. *Development.* 2002; 129: 1935–43.
39. **Reifers F, Walsh EC, Leger S, *et al.*** Induction and differentiation of the zebrafish heart requires fibroblast growth factor 8 (fgf8/acerebellar). *Development.* 2000; 127: 225–35.
40. **Abu-Issa R, Smyth G, Smoak I, *et al.*** Fgf8 is required for pharyngeal arch and cardiovascular development in the mouse. *Development.* 2002; 129: 4613–25.
41. **Dell'Era P, Ronca R, Coco L, *et al.*** Fibroblast growth factor receptor-1 is essential for *in vitro* cardiomyocyte development. *Circ Res.* 2003; 93: 414–20.
42. **Mohammadi M, McMahon G, Sun L, *et al.*** Structures of the tyrosine kinase domain of fibroblast growth factor receptor in complex with inhibitors. *Science.* 1997; 276: 955–60.
43. **Favata MF, Horiuchi KY, Manos EJ, *et al.*** Identification of a novel inhibitor of mitogen-activated protein kinase kinase. *J Biol Chem.* 1998; 273: 18623–32.
44. **Kuchera S, Barth H, Jacobson P, *et al.*** Anti-inflammatory properties of the protein kinase C inhibitor, 3-[1-[3-(dimethylamino) propyl]-1H-indol-3-yl]-4-(1H-indol-3-yl)-1H-pyrrole-2,5-dione monohydrochloride (GF109203X) in the PMA-mouse ear edema model. *Agents Actions.* 1993; 39 Spec No: C169–73.
45. **Chomczynski P, Sacchi N.** Single-step method of RNA isolation by acid guanidinium thiocyanate-phenol-chloroform extraction. *Anal Biochem.* 1987; 162: 156–9.
46. **Pfaffl MW, Horgan GW, Dempfle L.** Relative expression software tool (REST) for group-wise comparison and statistical analysis of relative expression results in real-time PCR. *Nucleic Acids Res.* 2002; 30: e36.
47. **Dell'Era P, Mohammadi M, Presta M.** Different tyrosine autophosphorylation requirements in fibroblast growth factor receptor-1 mediate urokinase-type plasminogen activator induction and mitogenesis. *Mol Biol Cell.* 1999; 10: 23–33.
48. **De Palma M, Naldini L.** Transduction of a gene expression cassette using advanced generation lentiviral vectors. *Methods Enzymol.* 2002; 346: 514–29.
49. **Magnusson PU, Ronca R, Dell'Era P, *et al.*** Fibroblast growth factor receptor-1 expression is required for hematopoietic but not endothelial cell development. *Arterioscler Thromb Vasc Biol.* 2005; 25: 944–9.
50. **Kiselyov VV, Kochoyan A, Poulsen FM, *et al.*** Elucidation of the mechanism of the regulatory function of the Ig1 module of the fibroblast growth factor receptor 1. *Protein Sci.* 2006; 15: 2318–22.
51. **Johnson DE, Williams LT.** Structural and functional diversity in the FGF receptor multigene family. *Adv Cancer Res.* 1993; 60: 1–41.
52. **Eswarakumar VP, Lax I, Schlessinger J.** Cellular signaling by fibroblast growth factor receptors. *Cytokine Growth Factor Rev.* 2005; 16: 139–49.
53. **Vincentz JW, Barnes RM, Firulli BA, *et al.*** Cooperative interaction of Nkx2.5 and Mef2c transcription factors during heart development. *Dev Dyn.* 2008; 237: 3809–19.
54. **Ericson J, Thor S, Edlund T, Jessell TM, Yamada T.** Early stages of motor neuron

differentiation revealed by expression of homeobox gene Islet-1. *Science.* 1992; 256: 1555–60.

55. **Chapman DL, Garvey N, Hancock S, *et al.*** Expression of the T-box family genes, Tbx1-Tbx5, during early mouse development. *Dev Dyn.* 1996; 206: 379–90.
56. **Alessi DR, Cuenda A, Cohen P, *et al.*** PD 098059 is a specific inhibitor of the activation of mitogen-activated protein kinase kinase *in vitro* and *in vivo*. *J Biol Chem.* 1995; 270: 27489–94.
57. **Thompson AK, Mostafapour SP, Denlinger LC, *et al.*** The aminosteroid U-73122 inhibits muscarinic receptor sequestration and phosphoinositide hydrolysis in SK-N-SH neuroblastoma cells. A role for Gp in receptor compartmentation. *J Biol Chem.* 1991; 266: 23856–62.
58. **Cuenda A, Rouse J, Doza YN, *et al.*** SB 203580 is a specific inhibitor of a MAP kinase homologue which is stimulated by cellular stresses and interleukin-1. *FEBS Lett.* 1995; 364: 229–33.
59. **Lu CW, Yabuuchi A, Chen L, *et al.*** Ras-MAPK signaling promotes trophectoderm formation from embryonic stem cells and mouse embryos. *Nat Genet.* 2008; 40: 921–6.
60. **Quinlan LR, Faherty S, Kane MT.** Phospholipase C and protein kinase C involvement in mouse embryonic stem-cell proliferation and apoptosis. *Reproduction.* 2003; 126: 121–31.
61. **Kook SH, Lee HJ, Chung WT, *et al.*** Cyclic mechanical stretch stimulates the proliferation of C2C12 myoblasts and inhibits their differentiation *via* prolonged activation of p38 MAPK. *Mol Cells.* 2008; 25: 479–86.
62. **Mohammadi M, Dionne CA, Li W, *et al.*** Point mutation in FGF receptor eliminates phosphatidylinositol hydrolysis without affecting mitogenesis. *Nature.* 1992; 358: 681–4.
63. **Besser D, Presta M, Nagamine Y.** Elucidation of a signaling pathway induced by FGF-2 leading to uPA gene expression in NIH 3T3 fibroblasts. *Cell Growth Differ.* 1995; 6: 1009–17.
64. **Schonwasser DC, Marais RM, Marshall CJ, *et al.*** Activation of the mitogen-activated protein kinase/extracellular signal-regulated kinase pathway by conventional, novel, and atypical protein kinase C isotypes. *Mol Cell Biol.* 1998; 18: 790–8.